An amphiphilic block copolymer-based colorimetric and fluorescent chemosensor for Hg^{2+} that was prepared, which was synthesized by sequential RAFT polymerizations of (NIPAM) and R6GDM (a novel Hg^{2+}-sensitive rhodamine monomer).

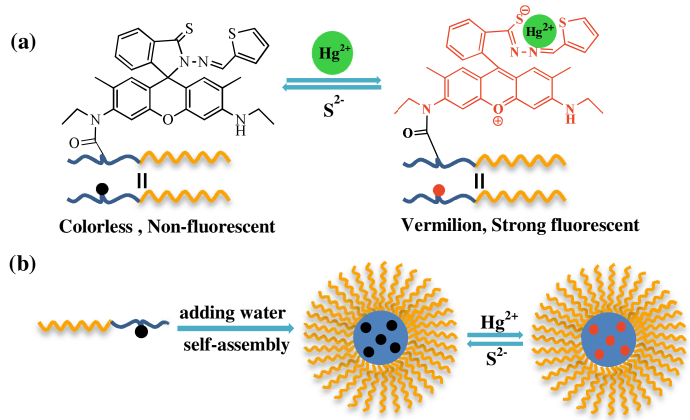

Analytical Methods

RSCPublishing

PAPER

Cite this: DOI: 10.1039/x0xx00000x

Hg^{2+}-selective chemosensor based on a novel amphiphilic block copolymer bearing rhodamine 6G derivative moieties self-assembly in purely aqueous media

Zhao Wang,*[a] Zhongkui Yang,[a] Tao Gao,[a] Jingwen He,[a] Laijiang Gong,[a] Yanbing Lu,[a] Yuanqin Xiong*[a] and Weijian Xu[a]

DOI: 10.1039/x0xx00000x

www.rsc.org/methods

We report on the fabrication of an amphiphilic block copolymer-based colorimetric and fluorescent chemosensor for Hg^{2+} ions that was prepared by sequential RAFT polymerizations of N-isopropylacrylamide (NIPAM) and a novel rhodamine-based Hg^{2+}-recognizing monomer, R6GDM. Because of its amphiphilic property, the block copolymer P[NIPAM]-b-P[R6GDM] can self-assemble into micelles, which allows it to be used as a chemosensor in aqueous solution. Upon addition of Hg^{2+} ions to the micelle solution, visual color change and fluorescence enhancement were observed. Moreover, it exhibits highly sensitive and selective for Hg^{2+} ions, relatively. Besides, it can serve as a potential multifunctional sensors to pH and temperature（at a specific temperature range: 25-40 ℃ or 40-52 ℃）. The water dispersibility and biocompatibility of these polymer micelles could provide a new strategy for detecting analytes in environmental and biological systems.

1 Introduction

Mercury contamination in the environment and in living organisms continues to be a critical issue of concern on a global scale. With the toxic effects of mercury on ecosystems and health well-established,[1] the need to detect mercury at extremely low concentrations persists.[2] Water-soluble Hg^{2+} is one of the most usual and stable form of mercury pollution due to its high toxicity and bioaccumulation.[3,4] Thus, routine detection of trace amounts of Hg^{2+} with high sensitivity and selectivity is central to environmental monitoring in aquatic ecosystems. In addition to the classic detection methods (such as CV-AAS, CV-AFS, ICP-MS) used for Hg^{2+} detection in water samples,[5] in the last few years, special attention has been paid to the use of electrochemical and optical sensors for selective and sensitive routine monitoring of mercury in water and biological samples,[6-16] because they are fast, cheap , highly sensitivity and selectivity. The use of optical sensors offers potential advantages over electrochemical ones such as electrical isolation, reduced noise interference, the possibility of miniaturization and remote sensing.[17] Among other methods, the fluorescence-based sensors represent a simple but sensitive technique for fast control of Hg^{2+} in many samples.[18]

Rhodamine-based fluorescent chemosensors for metal cations have enjoyed increasing interest in recent years by virtue of its excellent photophysical properties, such as long wavelength absorption and emission, high fluorescence quantum yield, large extinction coefficient, and high stability against light.[19-21] The on–off fluorescence switching of these chemosensors is based on structure change of the rhodamine moiety between spirocyclic and open ring forms. Without cations, these chemosensors exist in a spirocyclic form, which is colorless and non-fluorescent. In contrast, addition of metal cation leads to a spirocycle opening *via* coordination provides both chromogenic and fluorogenic responses that facilitate "naked eye" analyte detection.[6,11,22,23,26,30-32] Therefore, rhodamine-based derivatives have been widely used as sensing materials.[6,8,13,17,18,22-32] However, these rhodamine-based small molecule chemosensors typically exhibit poor water solubility and usually only function in a medium of pure organic solvent or an aqueous solution containing at least 50% organic cosolvent.[6,23,27,30-32] The lack of water solubility greatly limits the potential applications of rhodamine-based small molecules in biological systems and for environmental analyses.

To improve the water dispersibility of the organic dyes, the non-covalent[33-35] or covalent methods[12,36-38] incorporation of organic dyes into micelles have been reported, covalent methods means incorporating organic dyes into micelles by

[a] *College of Chemistry & Chemical Engineering, Hunan University, Changsha, China. Tel: +86-0731-88821549, E-mail addresses: wangzhao0724@163.com (Z. Wang), xyuanqin@sina.com (Y. Q. Xiong)*

† Electronic supplementary information (ESI) available.

attaching organic dyes to the backbone of the amphiphilic copolymers， because amphiphilic block copolymers can self-organize into core–shell micellar structures in aqueous solution and buried organic dyes in the hydrophobic core. However, to the best of our knowledge, there is no report about entirely use rhodamine-based derivatives as the hydrophobic block of amphiphilic block copolymers prepared by reversible addition-fragmentation chain transfer polymerization (RAFT) and its self-assembly into micelles as fluorescent chemosensors for Hg^{2+} in aqueous solution.

In this work, we report on the synthesis of an amphiphilic diblock copolymer P[NIPAM]-b-P[R6GDM], which is prepared by sequential RAFT polymerizations of a hydrophilic N-isopropylacrylamide (NIPAM) and a novel rhodamine 6G derivative Hg^{2+}-recognizing monomer, R6GDM. P[NIPAM]-b-P[R6GDM] could easily self-assemble into micelles in aqueous solution; a process that combines the advantages of the water dispersibility of the micelles and the metal-ion coordination ability of the rhodamine moiety to provide a novel type of Hg^{2+} ion probe. At the same time, we expected the thermo-sensitive block (PNIPAM) of P[NIPAM]-b-P[R6GDM] could improve detection sensitivities of Hg^{2+} ions and which can serve as multifunctional sensors. The experimental results showed that the P[NIPAM]-b-P[R6GDM] micelle selectively and sensitively reported the presence of Hg^{2+} in aqueous solution via a fluorescence “turn-on” and a visible color change.

Scheme 1. Proposed ring-opening mechanism for R6GDM in the presence of mercury(II) ions (a) and a schematic illustration of the formation of the P[NIPAM]-b-P[R6GDM] micelle and the mercury(II) ions sensing of the micelle in aqueous solution (b).

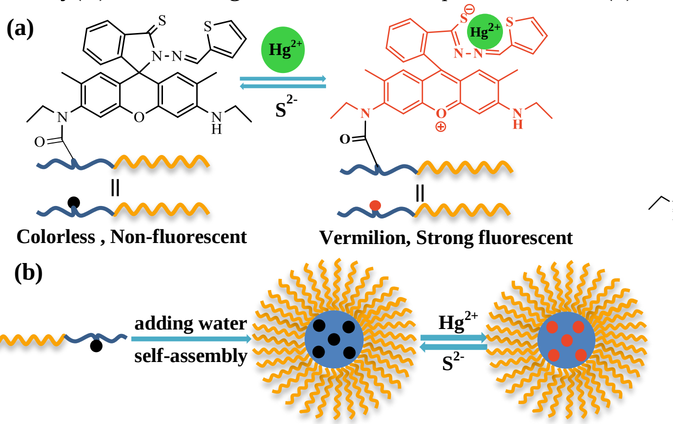

2 Experimental

2.1 Reagents and chemicals

Rhodamine 6G, Acryloyl chloride, 2-Thiophenecarboxaldehyde and Lawesson reagent were purchased from Aladdin Chemistry Co., Ltd., and used as received. N-Isopropylacrylamide (NIPAM, 98%, Aladdin) was recrystallized twice from a mixture of n-hexane and toluene (v/v =3:1) prior to use Triethylamine, anhydrous K_2CO_3, hydrazine hydrate, and all other reagents (Sinopharm Chemical Reagent Co.) were used as received. 2,2′-Azoisobutyronitrile (AIBN) was recrystallized from 95% ethanol, and dichloromethane (CH_2Cl_2) was dried and distilled prior to use. Dichloromethane (CH_2Cl_2) was dried over CaH_2 and distilled just prior to use. Toluene was distilled over sodium shavings and benzophenone immediately before use. Solutions of metal ions were prepared in distilled water from their corresponding nitrate salts (Na^+, K^+, Ag^+, Al^{3+}, Fe^{3+}, Ca^{2+}, Co^{2+}, Ba^{2+}, Mg^{2+}, Mn^{2+}, Ni^{2+}, Pb^{2+} and Zn^{2+}), except for $Hg(ClO_4)_2$ and $CuSO_4$. Water used for all the experiments which was deionized with a Milli-Q SP reagent water system.

2.2 Instrumentation and apparatus

The ^1H and ^{13}C NMR was acquired in $CDCl_3$ or d_6-DMSO on Varian INOVA-400 MHz NMR spectrometer using TMS as an internal standard. Gel permeation chromatography (GPC) of the obtained triblock copolymer was performed on a Waters 1515 GPC instrument in THF calibrated with standard polystyrene. Fluorescent spectra were recorded at room temperature with a HITACHI F-4600 fluorescence spectrophotometer with the excitation and emission slit widths at 5.0 and 5.0 nm respectively. Dynamic light scattering (DLS) measurements were carried out using a Nano-ZS90 zeta-potential and particle analyzer (Malvern, UK). Electrospray ionization mass spectra (ESI-MS) were obtained with a LCQ-Advantage spectrometer （Thermo Finnigan，USA）.

2.3 Sample Synthesis.

Synthetic schemes employed for the preparation of rhodamine 6G–based derivative sensitive and Hg^{2+}-recognizing fluorescent monomer (called R6GDM,**4**) and P[NIPAM]-b-P[R6GDM] are shown in Schemes 2 and 3.

Scheme 2. Synthetic schemes employed for the preparation of Hg^{2+}-recognizing rhodamine 6G-based fluorescent polymerizable monomer (R6GDM,**4**).

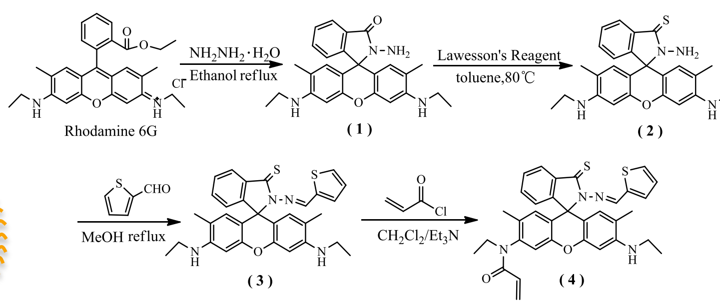

Scheme 3. Synthesis of amphiphilic thermoresponsive diblock copolymers, P[NIPAM]-b-P[R6GDM], via sequential RAFT polymerizations.

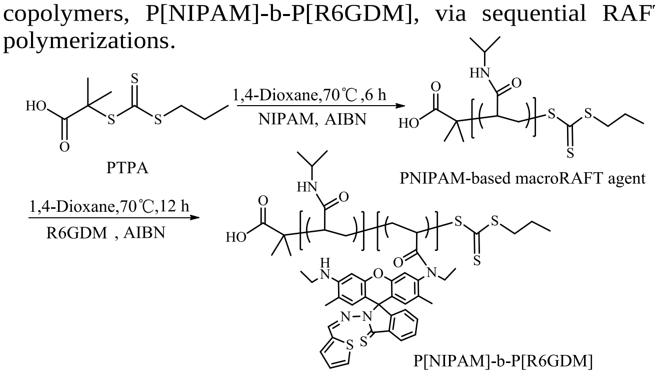

(a)Synthesis of the Rhodamine 6G hydrazide 1. Rhodamine-6G hydrazide is prepared according to the literature mothod.[39,40] In this work, Rhodamine-6G hydrazide was synthesized by a similar route as Yang's[31] Excess hydrazine hydrate (80%,15 mL) was added dropwise to a solution of rhodamine 6G (4.79 g, 10 mmol) in absolute ethanol (120 mL). After the addition, the resulting mixture was refluxed in an oil bath with stir for 10 h (pink precipitation could be observed soon after the mixture was heated). Then the precipitation was filtered, washed by ethanol (3 × 30 mL) and dried in vacuo to afford rhodamine 6G hydrazide (3.88 g, yield 81%) as light pink solid. ^{1}H NMR (400 MHz, d_6–DMSO) δ 7.79 – 7.71 (m, 1H), 7.53 – 7.37 (m, 2H), 6.94 (dd, J = 14.9, 12.1 Hz, 1H), 6.26 (s, 2H), 6.11 (d, J = 13.8 Hz, 2H), 5.03 (s, 2H), 3.12 (dd, J = 14.0, 6.9 Hz, 5H), 1.86 (s, 6H), 1.20 (t, J = 7.1 Hz, 6H).

(b) Synthesis of the Thiooxorhodamine-6G hydrazide 2: Thiooxorhodamine 6G hydrazide **1** is prepared according to the literature mothod.[26,41-43] In this work, Rhodamine 6G hydrazide (5.0 mmol, 2.14 g) and Lawesson's Reagent (5.0 mmol, 2.03 g) were dissolved in dry toluene (60 mL), the reaction mixture were heated at 80 ℃ for 24 h under N_2 atmosphere. After removal of toluene, the residue was stirred with K_2CO_3 concentrated for 2 h, and then extracted by CH_2Cl_2. After removal of CH_2Cl_2, the residue was purified by flash chromatography (ethyl acetate / petroleum, 6:1, R_f = 0.3) as eluent to afford Thiooxorhodamine 6G hydrazide (0.856 g, yield: 40%). R_f = 0.3 (SiO_2; ethyl acetate / petroleum, 6:1). ^{1}H NMR (400 MHz, $CDCl_3$) δ 8.12 (d, J = 7.1 Hz, 1H), 7.59 – 7.38 (m, 2H), 7.08 (d, J = 7.0 Hz, 1H), 6.41 (s, 2H), 6.13 (s, 2H), 4.83 (s, 2H), 3.22 (dd, J = 13.6, 6.6 Hz, 4H), 1.90 (s, 6H), 1.26 (s, 6H). ESI-MS: m/z 445.1 for $[M+H]^+$, calc. for $C_{26}H_{28}N_4OS$ = 444.2.

(c) Synthesis of the Thiooxorhodamine 6G thiophene Schiff base 3: Compound **3** is prepared according to the literature mothod.[6,8,26,42] Thiooxorhodamine 6G hydrazide (2.0 mmol, 0.888 g) and 2-thiophenecarboxaldehyde (6 mmol, 0.68 g) were dissolved in dry boiling methanol (40 mL), the reaction mixture were heated at 60 ℃ for 24 h under N_2 atmosphere. The white precipitates were filtered and washed with cold methanol and purified by flash chromatography (ethyl acetate / petroleum, 5:1, R_f = 0.3)(0.666 g, yield: 75%). ^{1}H NMR (400 MHz, $CDCl_3$) δ 8.72 (s, 1H), 8.38 – 8.30 (m, 1H), 8.26 – 8.07 (m, 1H), 7.77 – 7.68 (m, 1H), 7.56 – 7.33 (m, 4H), 7.18 – 7.02 (m, 2H), 6.64 (s, 1H), 6.58 (s, 1H), 6.28 (d, J = 7.5 Hz, 2H), 3.20 (q, J = 7.1 Hz, 4H), 1.91 (d, J = 2.4 Hz, 6H), 1.31 (t, J = 7.1 Hz, 6H). ESI-MS: m/z 539.1 for $[M+H]^+$, calc. for $C_{31}H_{30}N_4OS_2$ = 538.19.

(d) Synthesis of the monomer R6GDM 4

The monomer R6GDM was prepared by the reaction between Thiooxorhodamine 6G thiophene Schiff base **3** and acryloyl chloride in an ice bath according to the literature mothod.[6,44,45] To a 100 mL flask, the thiophene Schiff base (0.807g, 1.5 mmol) was dissolved in 30 mL of CH_2Cl_2, Et_3N was added (208 µL, 1.5 mmol) and the mixture was cooled in an ice bath. A solution of acryloyl chloride (122µL, 1.5 mmol) in CH_2Cl_2 (20 mL) was then added dropwise to the flask while stirring. All reagents and glass apparatuses were dried prior to use. After the addition of the reagents, the mixture was allowed stir in the cold ice bath for approximately 2 h, stirring was continued 12 h at room temperature and the solution was evaporated under vacuum. The residual red solid was purified by chromatography (ethyl acetate / petroleum, 6:1, R_f = 0.3), yellow powder was obtained (0.363 g, yield: 45%). ^{1}H NMR (400 MHz, $CDCl_3$) δ 8.74 (d, J = 4.1 Hz, 1H), 8.37 (d, J = 7.7 Hz, 1H), 8.18 (d, J = 2.8 Hz, 1H), 7.73 (d, J = 5.0 Hz, 1H), 7.65 – 7.35 (m, 3H), 7.12 (ddd, J = 22.0, 11.3, 6.1 Hz, 2H), 6.93 – 6.76 (m, 2H), 6.61 (dd, J = 19.6, 3.4 Hz, 1H), 6.36 (td, J = 17.1, 8.2 Hz, 2H), 6.06 – 5.78 (m, 1H), 5.51 (ddd, J = 12.3, 7.7, 1.9 Hz, 1H), 4.08 (dt, J = 13.6, 6.9 Hz, 1H), 3.21 (q, J = 7.1 Hz, 2H), 1.95 (d, J = 4.1 Hz, 6H), 1.40 – 1.21 (m, 6H). ESI-MS: m/z 593.2 for $[M+H]^+$, m/z 615.2 for $[M+Na]^+$, calc. for $C_{34}H_{32}N_4O_2S_2$ = 592.2 .

(e) Synthesis of PNIPAM-Based MacroRAFT Agent (Scheme 3). RAFT agent PTPA is prepared according to the literature mothod.[46] PNIPAM-based macroRAFT agent was prepared according to similar procedures reported previously.[48] Typical RAFT polymerization procedures employed for the synthesis of PNIPAM-based macroRAFT precursor are as follows. NIPAM (0.848 g, 7.2 mmol), PTPA (19 mg, 0.08 mmol), AIBN (2 mg, 12 µmol), and 1,4-dioxane (2 mL) were charged into a reaction tube equipped with a magnetic stirring bar. The tube was carefully degassed by three freeze pump thaw cycles and then sealed under vacuum. After thermostatting at 70 ℃ in an oil bath and stirring for 6 h, the reaction tube was quenched into the reaction tube was quenched into liquid nitrogen, opened, and diluted with THF; the mixture was then precipitated into an excess of cold diethyl ether. The above dissolution precipitation cycle was repeated for three times. After drying in a vacuum oven overnight at 30 ℃, PNIPAM-based macroRAFT agent was obtained as a yellowish powder (0.75 g, yield: 86.3%).

(f) Synthesis of P[NIPAM]-b-P[R6GDM] Amphiphilic Diblock Copolymer (Scheme 3).

Typical procedures[47] employed for the RAFT synthesis of P[NIPAM]-b-P[R6GDM], are as follows. Into a reaction tube equipped with a magnetic stirring bar, PNIPAM-based macroRAFT agent (140 mg, 16.1 µmol), R6GDM (62 mg, 0.105 mmol), AIBN (0.7 mg, 4.2 µmol), and 1,4-dioxane (1.2 mL) were charged. The tube was carefully degassed by three freeze -pump -thaw cycles and then sealed under vacuum. After thermostatting at 70 ℃ in an oil bath and stirring for 12 h, the reaction tube was quenched into the reaction tube was quenched into liquid nitrogen, opened, and diluted with THF; the mixture was then precipitated into an excess of cold diethyl ether. The above dissolution-precipitation cycle was repeated for three times. After drying in a vacuum oven overnight at 30 ℃, P[NIPAM]-b-P[R6GDM] was obtained as a reddish powder (122 mg, yield: 60.4%).

2.4 P[NIPAM]-b-P[R6GDM] self-assembled into micelles that were chemosensors in aqueous media

Micelles of P[NIPAM]-b-P[R6GDM] were prepared by a dialysis method.[45,47] Typical procedures employed for the preparation of micellar solutions are as follows. 20.0 mg of

P[NIPAM]-b-P[R6GDM] amphiphilic diblock copolymer was dissolved in 2 mL of DMF. Under vigorous stirring, 20 mL of deionized water was then slowly added. After the addition process is completed, the micellar solution was further stirred for another 4 h. DMF was then removed by dialysis (M_W cutoff, 5000 Da) against deionized water for 24 h. During this process, fresh deionized water was replaced approximately every 12 h. The final polymer concentration was adjusted by adding deionized water to 0.8 mg/mL.

2.5 Fluorescence measurement of the critical micelle concentration

The critical micelle concentration (cmc) of P[NIPAM]-b-P[R6GDM] was determined by a dye solubilization method using Nile Red (NR) as a probe molecule.[48,49] NR in THF (0.1 mg/mL, 30 μL) was added to a glass vial via a microsyringe. After THF was evaporated, a micellar solution (3 mL) was added. The concentration of the micellar solution was varied from 0.2 to 0.0001 mg/mL. Then the solution was stirred for 12 h. The fluorescence measurements were taken at an excitation wavelength of 560 nm and the emission was monitored from 580 nm to 750 nm.

3 Results and discussion

3.1 Synthesis of the monomer R6GDM

As shown in Scheme 2, the Hg^{2+}-recognizing monomer R6GDM was synthesized in four steps using rhodamine 6G as the starting material. [6,39-45] The structures of the compounds **1, 2, 3, 4** were confirmed by ^{1}H NMR, ^{13}C NMR and ESI-MS (Figure S1 to Figure S7, ESI†). Compound **4** is expected to act as a signal switcher, which is envisioned to turn on when the target cation is bound. [6,8,23,41] Upon the addition of Hg^{2+} ions, the spirolactam moiety of the rhodamine group opened (the formation of an open-ring structure), which resulted in the appearance of a vermilion color and an yellow fluorescence (Figure S13, ESI†).

3.2 Synthesis and characterization of P[NIPAM]-b-P[R6GDM]

P[NIPAM]-b-P[R6GDM] was synthesized by via sequential RAFT plymerizations of N-isopropylacrylamide (NIPAM) and the rhodamine-based Hg^{2+}-recognizing monomer, R6GDM (Scheme 3**)**, and P[NIPAM]-b-P[R6GDM] was synthesized. Because poly(N-isopropylacrylamide) (PNIPAM) is a biocompatible, water-soluble polymer with thermosensitivity, it has attracted attention as the hydrophilic block of amphiphilic block copolymers.[50-53] At the same time, we expected the the thermo-sensitive block (PNIPAM) could improve the probe performance, and endow the sensor temperature sensitive function. Thus, NIPAM was appropriately selected as the hydrophilic monomer. The structure of the obtained polymer was confirmed by ^{1}H NMR spectroscopy. The ^{1}H NMR spectra of PNIPAM-based macroRAFT agent and P[NIPAM]-b-P[R6GDM] in $CDCl_3$ are shown in Fig. 1. The characteristic NMR signals corresponding to the thiophene and benzene rings of R6GDM (δ(H) 6.0–9.0) appeared in the ^{1}H NMR spectrum of P[NIPAM]-b-P[R6GDM]. The molecular weight and molecular weight distribution of PNIPAM-based macroRAFT agent and P[NIPAM]-b-P[R6GDM] were determined by GPC using THF as the eluent, revealed that the former had a molecular weight (Mn) of 6006 and a polydispersity index (PDI) of 1.22, and the latter had a molecular weight (Mn) of 8653 and a polydispersity index (PDI) of 1.19 (Figure S9, ESI†). The degree of polymerization, DP, of PNIPAM-based macroRAFT agent was determined to be 75 by ^{1}H NMR analysis in $CDCl_3$. Thus, $P[NIPAM]_{75}$-b-$P[R6GBM]_5$ was obtained. R6GDM content in $P[NIPAM]_{75}$-b-$P[R6GBM]_5$ was determined to be 27 wt% (theoretical content: 30 wt%) by UV-vis spectroscopy by using R6GDM as the calibration standard (Figure S12, ESI†). As shown in Fig. 2， this observation confirmed that the hydrophobic functional monomer R6GDM had been successfully incorporated into the polymer,[45,54] and indicating that the spirolactam structure of rhodamine is predominant.

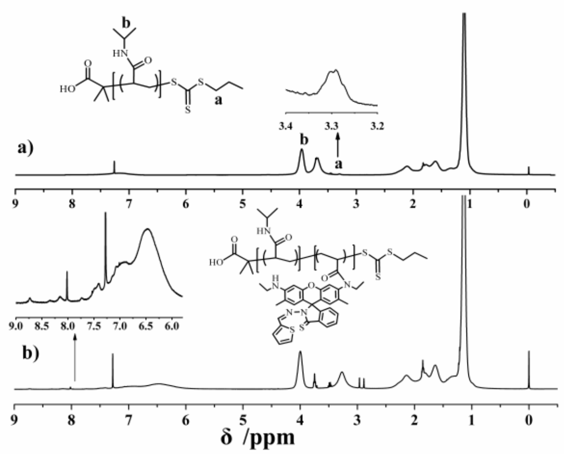

Fig. 1 ^{1}H NMR spectra of PNIPAM-based macroRAFT agent and $P[NIPAM]_{75}$-b-$P[R6GDM]_5$

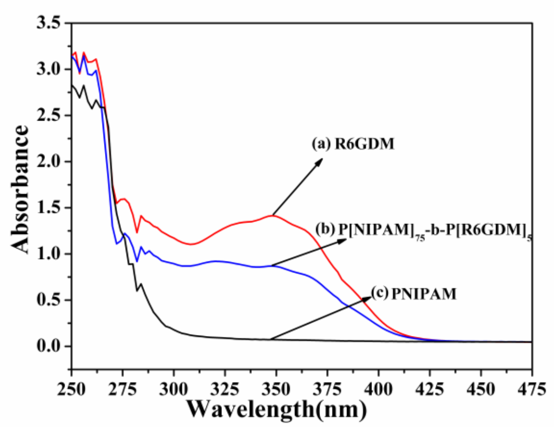

Fig. 2 Absorption spectra of (a) R6GDM (0.035 mg/mL), (b) $P[NIPAM]_{75}$-b-$P[R6GDM]_5$ (0.3 mg/mL) and (c) PNIPAM (0.5 mg/mL) in DMF solution.

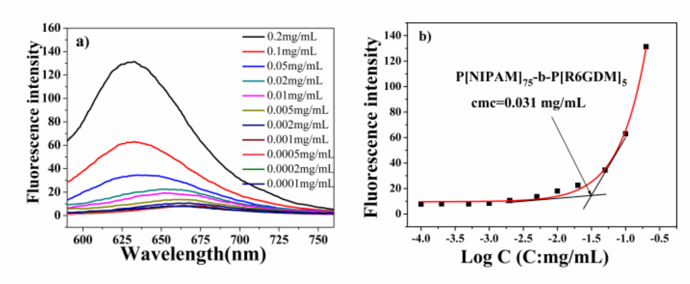

Fig. 3 Fluorescence emission spectra of Nile Red in P[NIPAM]$_{75}$-b-P[R6GDM]$_5$ of varying concentrations and their relevant emission intensity at 630 nm versus the log of concentration.

3.3 Self-assembling behavior of amphiphilic block copolymers P[NIPAM]$_{75}$-b-P[R6GDM]$_5$

The amphiphilic block copolymers P[NIPAM]$_{75}$-b-P[R6GDM]$_5$ self-assembled into micelles (Scheme 1), and their self-assembly behaviors were investigated in detail by means of fluorescence spectroscopy, DLS. Using hydrophobic Nile Red as a probe, fluorescence spectroscopy can conveniently monitor the micellar self-assembly and determine the critical micellar concentration (cmc) of the amphiphiles. As shown in Fig. 3, the emission fluorescence intensity gradually increased with increasing amphiphile concentration, suggesting the spontaneous self-assembly of micelles. The result shows the cmc of P[NIPAM]$_{75}$-b-P[R6GDM]$_5$ is 0.031 mg/ mL, and the cmc is relatively large, this can be ascribed to the short hydrophobic block P[R6GDM]. The size of the self-assembled micelles were then measured by DLS (Figure S11, ESI†), and the result showed that the micelles had an average diameter of approximately 106 nm (25 ℃) and 53 nm (50 ℃) with a narrow size distribution.

3.4 P[NIPAM]$_{75}$-b-P[R6GDM]$_5$ micelles as chemosensors for Hg^{2+} ions

3.4.1 Selectivity and sensitivity

The application of P[NIPAM]$_{75}$-b-P[R6GDM]$_5$ micelles as chemosensors for Hg^{2+} ions were investigated by fluorescence spectroscopies. As shown in Fig. 4a, the micelle solution showed almost no fluorescence in the absence of Hg^{2+} ions, indicating that the spirolactam structure of rhodamine is predominant. However, upon addition of Hg^{2+} ions, a visible color change occurred from colorless to vermilion (Figure S13, ESI†). With the addition of Hg^{2+} ions, a significant enhancement of fluorescence was observed that corresponded to the fluorescence emission of rhodamine 6G, and which shows the color change from colorless to orange that occurred when the micelle solutions were irradiated with UV light at 365 nm (Figure S13, ESI†). These changes are associated with the Hg^{2+}-induced spirolactam ring opening of the rhodamine group (Scheme 1a).

The selectivity of the P[NIPAM]$_{75}$-b-P[R6GDM]$_5$ micelle solution for common metal ions (Hg^{2+}, Fe^{3+}, Ag^+, Cu^{2+}, Al^{3+}, Pb^{2+}, Ni^{2+}, Co^{2+}, Mn^{2+}, Ca^{2+}, Ba^{2+}, Zn^{2+}, Mg^{2+}, K^+ and Na^+) was investigated by fluorescence measurements. As shown in (Fig. 4), it shows the fluorescence intensity change of the micelle solution in the presence of various ions; Hg^{2+} induced a considerable emission enhancement (~11.2-fold), whereas other metal ions produced a little fluorescence increase under identical conditions, with the exception of Fe^{3+}, Ag^+ and Cu^{2+}, which had slight enhancing effect (~2.88-fold), (~2.58-fold), (~1.84-fold), respectively. The signals of Hg^{2+} in the presence of other metal ions are also studied (Figure S14, ESI†). These results suggested that P[NIPAM]$_{75}$-b-P[R6GDM]$_5$ micelles can serve as a "naked-eye" and fluorescence sensor for Hg^{2+}.

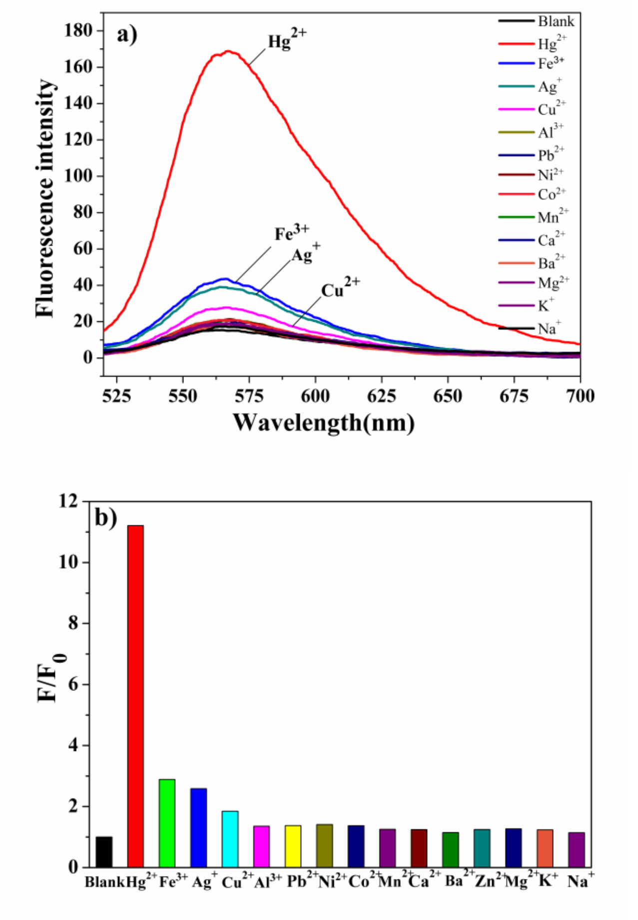

Fig. 4 (a) Fluorescence emission spectra and (b) relative fluorescence intensity (λ_{ex} = 500 nm, slit widths, excitation 5 nm, emission 5 nm; 25 ℃) recorded for the aqueous solution (pH 7) of P[NIPAM]$_{75}$-b-P[R6GDM]$_5$ (0.4 g/L, [R6GDM] = 47 μM) upon addition of 4.0 equiv (relative to R6GDM moieties) of various metal ions (Hg^{2+}, Fe^{3+}, Ag^+, Cu^{2+}, Al^{3+}, Pb^{2+}, Ni^{2+}, Co^{2+}, Mn^{2+}, Ca^{2+}, Ba^{2+}, Zn^{2+}, Mg^{2+}, K^+ and Na^+), respectively.

The Hg^{2+} interaction with P[NIPAM]$_{75}$-b-P[R6GDM]$_5$ at the low concentration region (0 ~ 8×10^{-8} M) showed nearly linear relation (Fig. 6). If we define the detection limit as the Hg^{2+} ions concentration at which a 10% fluorescence enhancement can be measured by employing 0.2 g/L aqueous solution of P[NIPAM]$_{75}$-b-P[R6GDM]$_5$,[37,52] the result shows Hg^{2+}-selective chemosensor P[NIPAM]$_{75}$-b-P[R6GDM]$_5$ with a detection limit of 6.89×10^{-9} M.

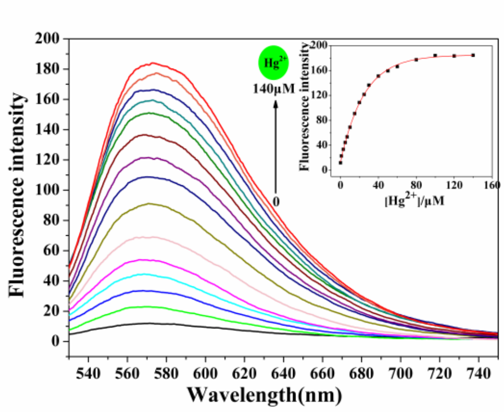

Fig. 5 Variation of relative fluorescence intensity (574 nm) of 0.4 g/L aqueous solution of P[NIPAM]$_{75}$-b-P[R6GDM]$_5$ (pH 7; λ_{ex} = 500 nm, slit widths: E_x=5 nm, E_m= 5 nm; [R6GDM] =47 μM) recorded at 25 ℃ upon gradual addition of Hg^{2+} (0 -140 μM), Inset: changes in the fluorescence intensity at 574 nm.

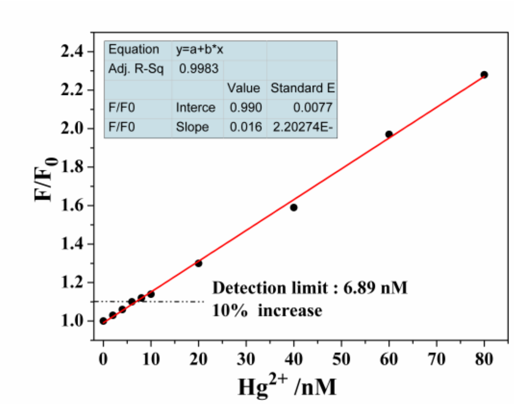

Fig. 6 Variation of relative fluorescence intensity (574 nm) of 0.2 g/L aqueous solution of P[NIPAM]$_{75}$-b-P[R6GDM]$_5$ (pH 7; λex = 500 nm, slit widths: Ex 5 nm, Em 5 nm) recorded at 25 ℃ upon gradual addition of Hg^{2+} (0 - 80nM), The detection limit was estimated to be 6.89 × 10^{-9} M.

3.4.2 Effects of pH and temperature

The influence of pH values on the fluorescence emission intensity of the fluorescent sensor in the absence of Hg^{2+} were studied by recording the fluorescence intensity at 574 nm over the pH range from 2 to 11. As can be seen from Fig. 7, the fluorescence emission intensity almost don't change with pH in the range of 7–11. However, when the pH of solution lower than 6, the fluorescence intensity of P[NIPAM]$_{75}$-b-P[R6GDM]$_5$ increased with pH reduced.[55] In addition, effect of pH to chemosensor P[NIPAM]$_{75}$-b-P[R6GDM]$_5$ is reversible (Figure S15, ESI†). Therefore, aqueous solution of P[NIPAM]$_{75}$-b-P[R6GDM]$_5$ could also serve as a potential sensor to pH .

Within P[NIPAM]$_{75}$-b-P[R6GDM]$_5$ micelles, P[NIPAM] and fluorescence emission off/on switchable R6GDM moieties are located in micellar coronas and cores, respectively. Thus, raised temperature can induce the collapse of P[NIPAM] coronas, which could enhance R6GDM emission due to the more hydrophobic microenvironment of P[R6GDM] cores at elevated temperatures; and this will enhance the fluorescence quantum yield of fluorescent reporters and achieve a signal amplification

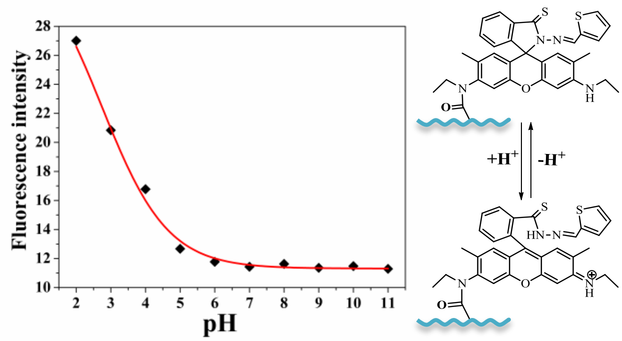

Fig. 7 Fluorescence emission spectra (λ_{ex}=500 nm, slit widths: E_x=5 nm, E_m=5 nm) recorded for 0.2 g/L aqueous solution (25 ℃) of P[NIPAM]$_{75}$-b-P[R6GDM]$_5$ in the pH range of 2 -11.

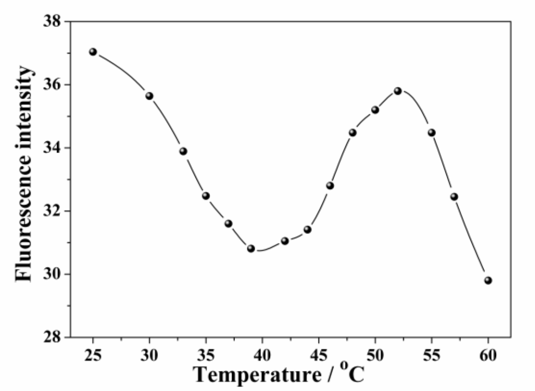

Fig. 8 Change in fluorescence intensity (λ_{ex} = 450 nm, slit widths: Ex. 5 nm, Em. 5 nm) recorded for 0.1 g/L aqueous solution of P[NIPAM]$_{75}$-b-P[R6GDM]$_5$ (pH 7 and 4 equiv. Hg^{2+}) in the temperature range of 25-60℃.

effect.[47,52] Fluorescence emission spectra obtained for the aqueous solution of P[NIPAM]$_{75}$-b-P[R6GDM]$_5$ upon addition of 4.0 equiv of Hg^{2+} in the temperature range of 25-60 ℃ are shown in Fig. 8. It was found that upon addition of Hg^{2+} ions in the temperature range of 25-40℃ the fluorescence emission intensity exhibits decrease, as compared to that at 25 ℃. The reason for this decrease is that, with the increase of temperature, the non-radiative deactivation rate enhancement, this process will lead to activation required activation energy increases, the fluorescence lifetime of the fluorescent substance decreased, then reduce the quantum yield of fluorescence substance.[56] The fluorescence enhancement was observed at a specific temperature range (40-52 ℃), which is almost in agreement with the lower critical solution temperature (LCST) obtained by temperature-dependent optical transmittance (Figure S10, ESI†),[47,52,57] and it basically reaches the expected effects. Interestingly, when temperature above 52 ℃, the fluorescence emission intensity of P[NIPAM]$_{75}$-b-P[R6GDM]$_5$ was decreased with increasing temperature. The explanation as follow, the thermo-induced collapse of P[NIPAM] coronas is a positive effect to the fluorescence emission intensity P[NIPAM]$_{75}$-b-P[R6GDM]$_5$, and raise the temperature leads to lower fluorescence quantum efficiency is a negative effect.

Thus, the two effects are competing against each other, when temperature above 52 ℃, the negative effect was greater than the positive one. Therefore, aqueous solution of P[NIPAM]$_{75}$-b-P[R6GDM]$_5$ could behaves as a potential T-sensing material at a specific temperature range: 25-40 ℃ or 40-52 ℃.

3.4.3 Response time , reversibility and binding stoichiometry

Besides high sensitivity and selectivity, a short response time is another necessity for a fluorescent chemosensor to dynamically monitor Hg^{2+} in environmental samples in real time. The recognition interaction of chemosensors P[NIPAM]$_{75}$-b-P[R6GDM]$_5$ was completed immediately after the addition of Hg^{2+} within 0.5 min (Fig. 9), compared to its analogues (which needed equilibrium time before detection).[12] Therefore, the chemosensors P[NIPAM]$_{75}$-b-P[R6GDM]$_5$ have potential to be used in real-time determination of Hg^{2+} in environmental and biological conditions.

For a chemical sensor , reversibility is important aspect that deserves attention. In the reversibility experiment, as excess of Na_2S were added into a solution of micellar sensor P[NIPAM]$_{75}$-b-P[R6GDM]$_5$ (0.4 mg/mL) + 4.0 equiv of Hg^{2+}, the color changed from vermilion to colorless and the fluorescent intensity was dramatically quenched, implying the decomplexation of Hg^{2+} by S^{2-} and a subsequent spirolactam ring closure reaction (Fig. 10). Further addition of Hg^{2+} still resulted in similar fluorescence changes. Thus, the polymer nanoparticles can be classified as reversible sensors for Hg^{2+}.

To determine the binding stoichiometry of R6GDM–Hg^{2+}, a Job's plot was measured with a total concentration of 50μM and the molar fraction of R6GDM from 0 to 1 (Fig. 11). As shown in the Job's plot, it can be observed that the fluorescence emission intensity reached a maximum at a molar fraction of about 0.5 of [R6GDM]/{[Hg^{2+}]+[R6GDM]}, indicating the 1 : 1 stoichiometry of Hg^{2+} and R6GDM.

3.5 Preliminary analytical applications

To test the practical application of Hg^{2+}-selective chemosensor P[NIPAM]$_{75}$-b-P[R6GDM]$_5$, tap and river waters (in which Hg^{2+} concentration was not detectable with the proposed method) were spiked with Hg^{2+} at different concentrations of 1 μM and 5 μM,[12,55,58] and analyzed with the proposed chemosensor P[NIPAM]$_{75}$-b-P[R6GDM]$_5$. The real water was pretreated by filtration before further determination. The results obtained are collected in Table 1 and show good agreement between the expected and found values. The results revealed that the Hg^{2+}-selective chemosensor P[NIPAM]$_{75}$-b-P[R6GDM]$_5$ could work in real water samples.

Table 1 Determination of Hg^{2+} in water samples using the proposed method

Water sample	Hg^{2+} spiked (μM)	Hg^{2+} recovered (μM) mean[a] ± SD[b]	Recovery (%)
Tap water 1	1.0	0.97 ±0.08	97
Tap water 2	5.0	5.13 ±0.13	102.6
River water 1	1.0	1.01 ±0.11	101.0
River water 2	5.0	5.21 ±0.09	104.2

[a]Mean of three determinations. [b]SD: standard deviation.

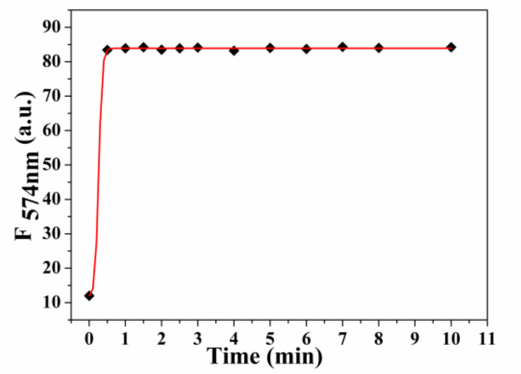

Fig. 9 Time evolution of P[NIPAM]$_{75}$-b-P[R6GDM]$_5$ (0.2 g/L, pH 7, 25 ℃) in the presence of 4.0 equiv of Hg^{2+} ion.

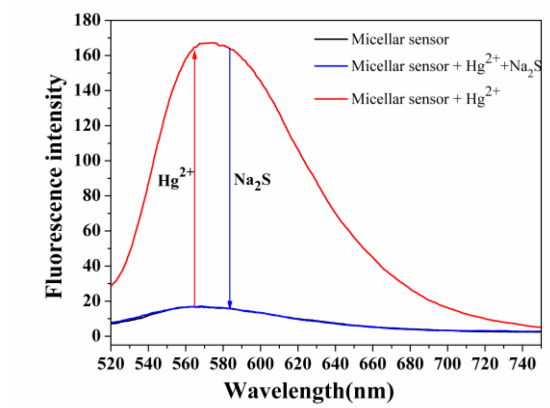

Fig. 10 Reversibility of Hg^{2+} ions to micellar sensor P[NIPAM]$_{75}$-b-P[R6GDM]$_5$ (0.4 mg/mL, pH 7, 25 ℃) by Na_2S. Red line: free micellar sensor (0.4 mg/mL), black line: micellar sensor + 4.0 equiv of Hg^{2+}, Blue line: micellar sensor + 4.0 equiv of Hg^{2+} + excess Na_2S (0.5 mM).

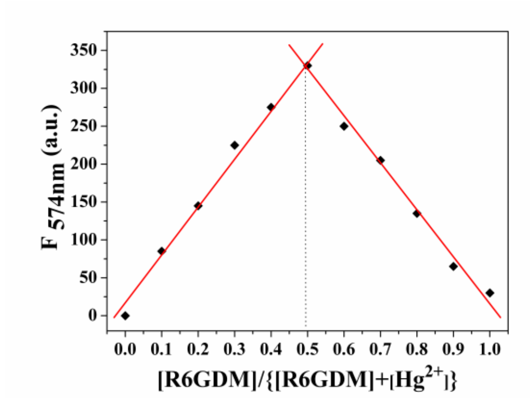

Fig. 11 Job's plot for R6GDM (forms 1 : 1 complexes) in aqueous ethanol (pH 7.0, 50 : 50, v/v) . The total concentration of R6GDM and Hg^{2+} is 50 μM.

4 Conclusion

In summary, an new amphiphilic block copolymer P[NIPAM]$_{75}$-b-P[R6GDM]$_5$ was synthesized by RAFT polymerizations, and the amphiphilic block copolymer self-assembled into micelles in aqueous solution, which can served as water-soluble chemosensors that selectively bind Hg^{2+} ions over other common metal ions, leading to an obvious color change and a considerable fluorescence enhancement. Moreover, which can serve as a potential multifunctional sensors to pH and temperature (at a specific temperature range: 25-40 ℃ or 40-52 ℃). In addition, the water dispersibility and biocompatibility of the micelles may provide a new approach for measuring Hg^{2+} ions in environmental and biological milieus.

Notes and references

1 F. Zahir, S. J. Rizwi, S. K. Haq and R. H. Khan, *Environ. Toxicol. Pharmacol.*, 2005, **20**, 351.
2 E. M. Nolan, S. J. Lippard, *Chem. Rev.*, 2008, **108**, 3443.
3 H. H. Harris, I. J. Pickering and G. N. George, *Science.*, 2003, **301**, 1203.
4 L. Onyido, A. R. Norris and E. Buncel, *Chem. Rev.*, 2004, **104**, 5911.
5 M. Leermakers, W. Baeyens, P. Quevauviller and M. Horvat, *Trends Anal. Chem.*, 2005, **24**, 383.
6 M. Suresh, S. Mishra, S. K. Mishra, E. Suresh, A. K. Mandal, A. Shrivastav and A . Das, *Org. Lett*., 2009. **11**, 2740.
7 X. H. Cheng, Q. Q. Li, J. G. Qin and Z. Li, *ACS Appl. Mater. Interfaces.*, 2010, **2**, 1066.
8 Y. Peng, , J. W. Zhou, L. Wu, E. H. Xiong, X. H. Zhang and J. H. Chen, *Electroanal Chem*., 2014, **732**, 61.
9 A. Thakur, S. Sardar and S. Ghosh, *Inorg. Chem.*, 2011, **50**, 7066.
10 E. S. Childress, C. A. Roberts and D. Y. Sherwood, *Anal. Chem.*, 2012, **84**, 1235.
11 Y. J. Gong, X. B. Zhang, C. C. Zhang and A. L. Luo, *Anal. Chem.*, 2012, **84**, 10777.
12 F. J. Orriach-Fernández, A. Medina-Castillo and J. F. Fernández-Sánchez, *Anal. Methods*., 2013, **5**, 6642.
13 K. Bera, A. K. Das and M. Nag, *Anal. Chem*., 2014, **86**, 2740.
14 P. Srivastava, S. S. Razi and R. Ali, *Anal. Chem*., 2014, **86**, 8693.
15 N. Zhang, Y. Si and Z. Sun, *Anal. Chem*., 2014, ***86***, 11714.
16 E. H. Xiong, L. Wu and J. Zhou, *Anal. Chim. Acta*., 2015, ***856***, 242.
17 J. F. Fernández-Sánchez, R. Cannas, S. Spichiger, R. Steiger and U. E. Spichiger-Keller, *Sens. Actuators, B.*, 2007, **128**, 145.
18 H. Li , L. Wang, *Analyst*., 2013, **138**, 1589.
19 Y. K. Yang, K. J. Yook and J. Tae, *J. Am. Chem. Soc*., 2005, **127**, 16760.
20 Y. Xiang, A. Tong, *Org. Lett*., 2006, **8**, 1549.
21 S. K. Ko, Y. K. Yang and J. Tae, *J. Am. Chem. Soc*., 2006, **128**, 14150.
22 Y. Zhao, X. B. Zhang and Z. X. Han, *Anal. Chem*., 2009, **81**, 7022.
23 Z. Jin, D. X. Xie and X. B. Zhang, *Anal. Chem*., 2012, **84**, 4253.
24 X. Q. Chen, T. Pradhan and J. Yoon, *Chem. Rev*., 2011, **112**, 1910.
25 M. Beija, C. A. Afonso and J. M. Martinho, *Chem. Soc. Rev*., 2009, **38**, 2410.
26 F. Wang, S. W. Nam and J. Yoon, *Sens. Actuators B.*, 2012, **161**, 948.
27 S. Park, W. Kim and J. Yoon, *Dyes Pigm*., 2013, **99**, 323.
28 K. V. Wu, H. D. Xiao and L. L. Wang, *RSC Adv*., 2014, **4**, 39984.
29 C. Kaewtong, N. Niamsa and B. Wanno, *New J. Chem*., 2014, **38**, 3831.
30 S. Lee, B. A. Rao and Y. A. Son, *Sens. Actuators B*., 2014, **196**, 388.
31 H. Y. Liu, X. J. Wan and Y. W. Yao, *Tetrahedron*, 2014, **70**, 7527.
32 Y. Yang, C. Y. Gao and L. M. Duan, *Sens. Actuators B*., 2014, **199**, 121.
33 Y. A. Diaz-Fernandez, E. Mottini, L. Pasotti, E. F. Craparo and G. Giammona, *Biosens. Bioelectron*., 2010, **26**, 29..
34 J. Chen, F. Zeng and S. Wu, *ChemPhysChem*., 2010, **11**, 1036.
35 B. Ma, M. Xu, F. Zeng and L. Huang, *Nanotechnology*., 2011, **22**, 065501.
36 X. J. Wan, T. Liu and S. Y. Liu, *Langmuir*., 2011, **27**, 4082.
37 T. Liu, S. Y. Liu, *Anal. Chem*., 2011, **83**, 2775.
38 Y. Qi, N. Li, Q. Xu, X. Xia, J. Ge and J. Lu, *React. Funct. Polym*., 2011, **71**, 390.
39 Y. K. Yang, K. J. Yook and J. Tae , *J. Am. Chem. Soc*., 2005, **127,** 16760.
40 X. F. Yang, X. Q. Guo and Y. B. Zhao, *Talanta*., 2002, **57**, 883.
41 Y. Zhou, X. Y. You , Y. Fang, J. Y. Li , K. Liu and C. Yao, *Org. Biomol. Chem*., 2010, **8**, 4819.
42 W. Huang, C. Song, C. He, G. Lv, X. Hu, X. Zhu and C. Duan, *Inorg. Chem*., 2009, **48**, 5061.
43 S. J. Coats, J. S. Link and D. J. Hlasta, *Org. Lett*., 2003. **5**, 721.
44 M. Calmes, J. Daunis, H. Ismaili, R. Jacquier, J. Koudou, G. Nkusi and A. Zouanate, *Tetrahedron*., 1990. **46**, 6021.
45 Y. Wang, H. Wu and J. Luo, *React. Funct. Polym*., 2012, **72**, 169.
46 Z. An, W. Tang, M. Wu, Z. Jiao and G. D. Stucky, *Chem. Commun*., 2008, **48**, 6501.
47 J. M. Hu, L. Dai and S . Y. Liu, *Macromolecules*., 2011, **44**, 4699.
48 R. C. Pratt, B. G. Lohmeijer, D. A. Long, P. P. Lundberg, A. P. Dove, H. Li and J. L. Hedrick, *Macromolecules*., 2006, **39**, 7863.
49 D. Hu, Y. F. Li and Y. L. Niu, *RSC Adv*., 2014, **4**, 47929.
50 A. J. Convertine, B. S. Lokitz, Y. Vasileva, L. J. Myrick, C. W. Scales, A. B. Lowe and C. L. McCormick, *Macromolecules*., 2006, **39**, 1724.
51 B. S. Lokitz, A. J. Convertine, R. G. Ezell, A. Heidenreich, Y. Li and C. L. McCormick, *Macromolecules.*, 2006, **39**, 8594.
52 J. M. Hu, C. H. Li and S. Y. Liu, *Langmuir*., 2009, **26**, 724.
53 Y. Wu, H. Hu, J. Hu, T. Liu, G. Zhang and S. Liu, *Langmuir*., 2013, **29**, 3711.
54 G. J. He, D. Guo, C. He, X. L. Zhang, X .W. Zhao and C. Y. Duan, *Angew. Chem. Int. Ed*., 2009, **48**, 6132.
55 C. H. Ma, L. P. Lin, Y. Y. Du, L. B. Chen, F. Luo and X. Chen, *Anal. Methods*., 2013, **5**, 1843.
56 Z. C. Cui, W. Q .Liu and N. J. Zhao, *Spectrosc. Spectr Anal*, 2006, **26**, 1127.
57 Y. Shiraishi, R. Miyamoto and X. Zhang, *Org. Lett*., 2007, **9**, 3921.
58 C. B. Gong, D. Jiang and Q. Tang, *Anal. Methods*., 2014, **6**, 7601.

